

**PREPARATION OF ACTIVATED CARBON FROM PINEAPPLE PEEL
AND POMELO PEEL FOR DYES REMOVAL: EQUILIBRIUM, KINETIC
AND THERMODYNAMIC STUDIES**

by

NUR AYSHAH ROSLI

**Thesis submitted in fulfillment of the requirements
for the degree of
Master of Science**

August 2012

ACKNOWLEDGEMENT

First of all, I would like to thank my parents and family for their endless support, love, and encouragement throughout my studies. They have made me more confident to face the challenge especially during the project progression. Special thanks to Assoc. Prof. Dr. Mohd Azmier Ahmad as my supervisor for this project. He was very supportive and willingly shared his time and knowledge with me without any hesitation. I would also like to thank him for giving me adequate freedom and flexibility while working on this project.

I would like to further my special thanks to Mr. Roqib, Mr. Syamsul Hidayat, Mr. Faiza, Mr. Ismail and Mrs. Latiffah for their technical guidance and support towards my experimental work in the laboratories at School of Chemical Engineering. I would like to take this opportunity to convey my gratitude and appreciation to my fellow post graduate students, for sharing their knowledge, professional advices and guidelines throughout the whole project. Useful discussions and suggestions from them are deeply appreciated. Special thanks to my dearest friends for their guidance and kindness help they have given to me. Last but not least, I would like to express deepest gratitude to those who have directly and indirectly contributed to the accomplishment and outcome of this project. Thank you so much.

Nur Ayshah Rosli

August 2012

TABLE OF CONTENTS

	Page
ACKNOWLEDGEMENT	ii
TABLE OF CONTENTS	iii
LIST OF TABLES	vii
LIST OF FIGURES	xii
LIST OF PLATES	xviii
LIST OF SYMBOLS	xix
LIST OF ABBREVIATIONS	xxii
ABSTRAK	xxiii
ABSTRACT	xxv
CHAPTER ONE: INTRODUCTION	
1.1 Dyes in textile industries	1
1.2 Agricultural waste based adsorbent	2
1.3 Problem statement	4
1.4 Scope of study	4
1.5 Research objectives	6
1.6 Organization of thesis	6
CHAPTER TWO: LITERATURE REVIEW	
2.1 Dyes wastewater treatment	8
2.2 Activated carbon precursor	10
2.2.1 Pineapple (<i>Ananas comosus L.</i>) peel	12
2.2.2 Pomelo (<i>Citrus grandis L.</i>) peel	13
2.3 Preparation method of activated carbon from agricultural waste	14
2.4 Influence of preparation variable to activated carbon	15
2.5 Optimization of preparation condition of activated carbon	17
2.6 Characterization of activated carbon	18
2.6.1 Activated carbon yield	19
2.6.2 Surface area and pore characteristics	19
2.6.3 Surface morphology	20
2.6.4 Proximate analysis	22
2.6.5 Surface chemistry	22

2.7	Adsorption isotherm	23
2.7.1	Langmuir isotherm	24
2.7.2	Freundlich isotherm	25
2.7.3	Temkin isotherm	26
2.7.4	Koble-corrigan isotherm	26
2.7.5	Toth isotherm	26
2.7.6	Sips isotherm	27
2.7.7	Vieth-Sladek isotherm	27
2.7.8	Radke-Prausnitz isotherm	28
2.7.9	Buoers-Sotolongo isotherm	28
2.8	Adsorption kinetic	28
2.8.1	Pseudo-first-order kinetic model	29
2.8.2	Pseudo-second-order kinetic model	29
2.8.3	Elovich kinetic model	30
2.8.4	Avrami kinetic model	30
2.8.5	Intraparticle diffusion model	31
2.8.6	Validity of kinetic model	32
2.9	Adsorption thermodynamic	32

CHAPTER THREE: MATERIALS AND METHOD

3.1	Materials	34
3.2	General description of equipment	36
3.2.1	Activated carbon preparation	36
3.2.2	Batch adsorption system and analysis system	38
3.2.3	Characterization system	39
3.3	Experimental procedure	40
3.3.1	Precursor preparation	40
3.3.2	Activated carbon preparation	40
3.3.2(a)	Carbonization	41
3.3.2(b)	KOH impregnation	41
3.3.2(c)	Carbon dioxide gasification	41
3.3.3	Experimental design	42
3.3.4	Batch equilibrium studies	45
3.3.4(a)	Effect of initial adsorbate concentration and contact time	45
3.3.4(b)	Effect of solution temperature	46
3.3.4(c)	Effect of solution pH	46
3.3.4(d)	Adsorption isotherm	46
3.3.5	Batch kinetic studies	47
3.3.6	Adsorption thermodynamics	47
3.3.7	Experimental activities	49

CHAPTER FOUR: RESULT AND DISCUSSION

4.1	Experimental design	50
4.1.1	Preparation of PiPAC using design of experiment	50
4.1.1 (a)	Development of regression model equation for preparation of PiPAC	50
4.1.1 (b)	MB removal of PiPAC	57
4.1.1 (c)	MR removal of PiPAC	59
4.1.1 (d)	RBV removal of PiPAC	60
4.1.1 (e)	PiPAC yield	62
4.1.2	Preparation of PoPAC using design of experiment	63
4.1.2 (a)	Development of regression model equation for preparation of PoPAC	65
4.1.2 (b)	MB removal of PoPAC	69
4.1.2 (c)	MR removal of PoPAC	70
4.1.2 (d)	RBV removal of PoPAC	72
4.1.2 (e)	PoPAC yield	72
4.1.3	Optimization of operating parameters	73
4.2	Characterization of activated carbons	77
4.2.1	Surface area and pore characteristics	77
4.2.2	Surface morphology	78
4.2.3	Proximate analysis	80
4.2.4	Surface chemistry	80
4.3	Batch adsorption studies of methylene blue, methyl red, and remazol brilliant violet 5R onto PiPAC and PoPAC	85
4.3.1	Batch equilibrium studies	85
4.3.1 (a)	Effect of contact time and initial concentration of adsorbate	85
4.3.1 (b)	Effect of solution temperature	92
4.3.1 (c)	Effect of initial pH	94
4.3.2	Adsorption Isotherm	97
4.3.2 (a)	Methylene blue adsorption isotherm	97
4.3.2 (b)	Methyl red adsorption isotherm	101
4.3.2 (c)	Remazol brilliant violet 5R adsorption isotherm	105
4.3.3	Batch kinetics studies	109
4.3.3 (a)	Methylene blue adsorption kinetics and diffusion mechanism	109
4.3.3 (b)	Methyl red adsorption kinetics and diffusion mechanism	118
4.3.3 (c)	Remazol brilliant violet 5R adsorption kinetics and diffusion mechanism	127
4.3.4	Adsorption thermodynamics behaviours	135

CHAPTER FIVE: CONCLUSION AND RECOMMENDATION

5.1	Conclusions	139
5.2	Recommendations	141

REFERENCES	142
-------------------	------------

APPENDICES

Appendix A	153
Appendix B	155
Appendix C	161
Appendix D	173
Appendix E	176
Appendix F	188
Appendix G	194

LIST OF TABLES

Table 2.1	Principal existing and emerging processes for dye removal	9
Table 2.2	Adsorption capacities for activated carbons derived from agricultural wastes	11
Table 2.3	Physical characteristics of activated carbon produced from various precursors	20
Table 2.4	FTIR spectrum band assignments for pistachio-nut shell activated carbon	23
Table 3.1	List of chemicals	34
Table 3.2	Properties of methylene blue	35
Table 3.3	Properties of methyl red	35
Table 3.4	Properties of remazol brilliant violet 5R	36
Table 3.5	Independent variables and their coded levels for the CCD	42
Table 3.6	Experimental design matrixes	43
Table 4.1	Matrix for preparation of PiPAC	51
Table 4.2	ANOVA analysis for MB removal for PiPAC	54
Table 4.3	ANOVA analysis for MR removal for PiPAC	54
Table 4.4	ANOVA analysis for RBV removal for PiPAC	55
Table 4.5	ANOVA analysis for PiPAC yield	56
Table 4.6	Matrix for preparation of PoPAC	64
Table 4.7	ANOVA analysis for MB removal for PoPAC	66
Table 4.8	ANOVA analysis for MR removal for PoPAC	67
Table 4.9	ANOVA analysis for MR removal for PoPAC	68
Table 4.10	ANOVA analysis for PoPAC yield	68
Table 4.11	Model validation for activated carbons prepared for MB removal	76
Table 4.12	Model validation for activated carbons prepared for MR removal	76
Table 4.13	Model validation for activated carbons prepared for RBV removal	76
Table 4.14	Surface area and pore characteristics of the prepared activated carbons	77

Table 4.15	Proximate analysis for the prepared activated carbons	80
Table 4.16	FTIR spectrum band assignments for PiP, PiP char and PiPAC	81
Table 4.17	FTIR spectrum band assignments for PoP, PoP char and PoPAC	82
Table 4.18	Isotherm parameters for PiPAC-MB at temperature 30°C	100
Table 4.19	Isotherm parameters for PoPAC-MB at temperature 30°C	100
Table 4.20	Isotherm parameters for PiPAC-MR at temperature 30°C	104
Table 4.21	Isotherm parameters for PoPAC-MR at temperature 30°C	104
Table 4.22	Isotherm parameters for PiPAC-RBV at temperature 30°C	108
Table 4.23	Isotherm parameters for PoPAC-RBV at temperature 30°C	108
Table 4.24	Kinetic model constant parameter for adsorption of PiPAC-MB at 30°C	112
Table 4.25	Kinetic model constant parameter for adsorption of PoPAC-MB at 30°C	114
Table 4.26	Intraparticle diffusion model constant and correlation coefficient for adsorption of MB onto PiPAC-MB and PoPAC-MB at 30°C	117
Table 4.27	Kinetic model constant parameter for adsorption of PiPAC-MR at 30°C	121
Table 4.28	Kinetic model constant parameter for adsorption of PoPAC-MR at 30°C	121
Table 4.29	Intraparticle diffusion model constant and correlation coefficient for adsorption of MR onto PiPAC-MR and PoPAC-MR at 30°C	125
Table 4.30	Kinetic model constant parameter for adsorption of PiPAC-RBV at 30°C	129
Table 4.31	Kinetic model constant parameter for adsorption of PoPAC-RBV at 30°C	130
Table 4.32	Intraparticle diffusion model constant and correlation coefficient for adsorption of RBV onto PiPAC-RBV and PoPAC-RBV at 30°	134
Table 4.33	Thermodynamic parameters for adsorption of MB, MR and RBV onto PiPAC and POAC	137
Table C1	Isotherm parameters for PiPAC-MB at temperature 45°C	163
Table C2	Isotherm parameters for PiPAC-MB at temperature 60°C	163

Table C3	Isotherm parameters for PoPAC-MB at temperature 45°C	164
Table C4	Isotherm parameters for PoPAC-MB at temperature 60°C	164
Table C5	Isotherm parameters for PiPAC-MR at temperature 45°C	167
Table C6	Isotherm parameters for PiPAC-MR at temperature 60°C	167
Table C7	Isotherm parameters for PoPAC-MR at temperature 45°C	168
Table C8	Isotherm parameters for PoPAC-MR at temperature 60°C	168
Table C9	Isotherm parameters for PiPAC-RBV at temperature 45°C	171
Table C10	Isotherm parameters for PiPAC-RBV at temperature 60°C	171
Table C11	Isotherm parameters for PoPAC-RBV at temperature 45°C	172
Table C12	Isotherm parameters for PoPAC-RBV at temperature 60°C	172
Table E1	Kinetic model constant parameter for adsorption of PiPAC-MB at 45°C	176
Table E2	Kinetic model constant parameter for adsorption of PiPAC-MB at 60°C	177
Table E3	Kinetic model constant parameter for adsorption of PoPAC-MB at 45°C	178
Table E4	Kinetic model constant parameter for adsorption of PoPAC-MB at 60°C	179
Table E5	Kinetic model constant parameter for adsorption of PiPAC-MR at 45°C	180
Table E6	Kinetic model constant parameter for adsorption of PiPAC-MR at 60°C	181
Table E7	Kinetic model constant parameter for adsorption of PoPAC-MR at 45°C	182
Table E8	Kinetic model constant parameter for adsorption of PoPAC-MR at 60°C	183
Table E9	Kinetic model constant parameter for adsorption of PiPAC-RBV at 45°C	184
Table E10	Kinetic model constant parameter, correlation coefficient and normalized standard deviation values for adsorption of PiPAC-RBV at 60°C	185

Table E11	Kinetic model constant parameter for adsorption of PoPAC-RBV at 45°C	186
Table E12	Kinetic model constant parameter for adsorption of PoPAC-RBV at 60°C	187
Table F1	Intraparticle diffusion model and correlation coefficients for adsorption of MB onto PiPAC-MB and PoPAC-MB at 45°C	189
Table F2	Intraparticle diffusion model and correlation coefficients for adsorption of MB onto PiPAC-MB and PoPAC-MB at 60°C	189
Table F3	Intraparticle diffusion model and correlation coefficients for adsorption of MR onto PiPAC-MR and PoPAC-MR at 45°C	190
Table F4	Intraparticle diffusion model and correlation coefficients for adsorption of MR onto PiPAC-MR and PoPAC-MR at 60°C	191
Table F5	Intraparticle diffusion model and correlation coefficients for adsorption of RBV onto PiPAC-RBV and PoPAC-RBV at 45°C	192
Table F6	Intraparticle diffusion model and correlation coefficients for adsorption of RBV onto PiPAC-RBV and PoPAC-RBV at 60°C	193

LIST OF FIGURES

Figure 3.1	Schematic diagram of the experimental setup for activated carbon production	37
Figure 3.2	Schematic flow diagrams of experimental activities	49
Figure 4.1	Predicted versus experimental for (a) MB removal; (b) MR removal; (c) RBV removal; and (d) PiPAC yield	57
Figure 4.2	Response surface plot of MB removal (Effect of activation temperature and activation time, IR = 2.25) of PiPAC	59
Figure 4.3	Response surface plot of MR removal (Effect of activation temperature and impregnation ratio, activation time = 2 hours) of PiPAC	60
Figure 4.4	Response surface plot of RBV removal (Effect of activation temperature and IR, activation time = 2 hours) of PiPAC	61
Figure 4.5	Response surface plot of PiPAC yield (Effect of activation temperature and activation time, IR = 2.25)	63
Figure 4.6	Predicted versus experimental for (a) MB removal; (b) MR removal; (c) RBV removal; and (d) PoPAC yield	69
Figure 4.7	Response surface plot of MB removal (Effect of activation temperature and activation time, IR = 2.25) of PoPAC	70
Figure 4.8	Response surface plot of MR removal (Effect of activation temperature and IR, activation time = 2.00 hr) of PoPAC	71
Figure 4.9	Response surface plot of RBV removal (Effect of activation temperature and IR, activation time = 2 hours) of PoPAC	72
Figure 4.10	Response surface plot of PoPAC yield (Effect of activation temperature and activation time, IR = 2.25)	73
Figure 4.11	FTIR spectrums; (a) PiP; (b) PiP char; and (c) PiPAC	83
Figure 4.12	FTIR spectrums; (a) PoP; (b) PoP char; and (c) PoPAC	84

Figure 4.13	MB adsorption uptakes versus adsorption time at various initial concentrations at 30°C, (a) PiPAC-MB; and (b) PoPAC-MB	87
Figure 4.14	MB percent removals versus adsorption time at various initial concentrations at 30°C, (a) PiPAC-MB; and (b) PoPAC-MB	87
Figure 4.15	MR adsorption uptake versus adsorption time at various initial concentrations at 30 °C on (a) PiPAC-MR; and (b) PoPAC-MR	90
Figure 4.16	MR percent removal versus adsorption time at various initial concentrations at 30 °C on (a) PiPAC-MR; and (b) PoPAC-MR	90
Figure 4.17	RBV adsorption uptake versus adsorption time at various initial concentrations at 30 °C on (a) PiPAC-RBV; and (b) PoPAC-RBV	91
Figure 4.18	RBV percent removal versus adsorption time at various initial concentrations at 30 °C on (a) PiPAC-RBV; and (b) PO-RBV	91
Figure 4.19	Effect of solution temperature on MB adsorption capacity of PiPAC-MB and PoPAC-MB	93
Figure 4.20	Effect of solution temperature on MR adsorption capacity of PiPAC- MR and PoPAC-MR	94
Figure 4.21	Effect of solution temperature on RBV adsorption capacity of PiPAC- RBV and PoPAC-RBV	94
Figure 4.22	Effect of initial pH on MB removal on PiPAC-MB and PoPAC-MB	95
Figure 4.23	Effect of initial pH on MR removal on PiPAC-MR and PoPAC-MR	86
Figure 4.24	Effect of initial pH on RBV removal on PiPAC-RBV and PoPAC-RBV	97
Figure 4.25	Graph of adsorption isotherm models for PiPAC-MB at temperature 30°C	99
Figure 4.26	Graph of adsorption isotherm models for PoPAC-MB at temperature 30°C	99
Figure 4.27	Plots of separation factor versus MB initial concentration for adsorption of PiPAC-MB and PoPAC-MB at 30°C	101
Figure 4.28	Graph of adsorption isotherm models for PiPAC-MR at temperature 30°C	103
Figure 4.29	Graph of adsorption isotherm models for PoPAC-MR at temperature 30°C	103

Figure 4.30	Plots of separation factor versus MR initial concentration for adsorption of PiPAC-MR and PoPAC-MR at 30°C	105
Figure 4.31	Graph of adsorption isotherm models for PiPAC-RBV at temperature 30°C	107
Figure 4.32	Graph of adsorption isotherm models for PoPAC-RBV at temperature 30°C	107
Figure 4.33	Plots of separation factor versus RBV initial concentration for adsorption of PiPAC-RBV and PoPAC-RBV at 30°C	108
Figure 4.34	Linerized plots of (a) pseudo-first-order; (b) pseudo-second-order; (c) Elovich; and (d) Avrami kinetic model for MB adsorption onto PiPAC-MB at 30°C	111
Figure 4.35	Linerized plots of (a) pseudo-first-order; (b) pseudo-second-order; (c) Elovich; and (d) Avrami kinetic model for MB adsorption onto PiPAC-MB at 30°C	113
Figure 4.36	Plots of intraparticle diffusion model for MB adsorption onto (a) PiPAC-MB and (b) PoPAC-MB at 30 °C	115
Figure 4.37	Boyd plots for adsorption of MB onto (a) PiPAC-MB and (b) PoPAC-MB at 30 °C	118
Figure 4.38	Linerized plots of (a) pseudo-first-order; (b) pseudo-second-order; (c) Elovich; and (d) Avrami kinetic model for MR adsorption onto PiPAC at 30°C	120
Figure 4.39	Linerized plots of (a) pseudo-first-order; (b) pseudo-second-order; (c) Elovich; and (d) Avrami kinetic model for MR adsorption onto PoPAC at 30°C	122
Figure 4.40	Plots of intraparticle diffusion model for MR adsorption onto (a) PiPAC-MR and (b) PoPAC-MR at 30 °C	124
Figure 4.41	Boyd plots for adsorption of MR onto (a) PiPAC-MR and (b) PoPAC-MR at 30 °C	126
Figure 4.42	Linerized plots of (a) pseudo-first-order; (b) pseudo-second-order; (c) Elovich; and (d) Avrami kinetic model for RBV adsorption onto PiPAC at 30°C	128
Figure 4.43	Linerized plots of (a) pseudo-first-order; (b) pseudo-second-order; (c) Elovich; and (d) Avrami kinetic model for RBV adsorption onto PoPAC at 30°C	131
Figure 4.44	Plots of intraparticle diffusion model for RBV adsorption onto (a) PiPAC-RBV and (b) PoPAC-RBV at 30 °C	133

Figure 4.45	Boyd plots for adsorption of RBV onto (a) PiPAC-RBV and (b) PoPAC-RBV at 30 °C	135
Figure 4.46	Plots of $\ln k_2$ versus $1/T$ adsorption of MB, MR and RBV onto PiPAC and PoPAC	136
Figure 4.47	Plots of $\ln k_L$ versus $1/T$ for adsorption of MB, MR and RBV onto PiPAC and PoPAC	137
Figure A1	Calibration curve of methylene blue	153
Figure A2	Calibration curve of methyl red	153
Figure A3	Calibration curve of remazol brilliant violet 5R	154
Figure B1	MB adsorption uptake versus adsorption time at various initial concentrations at 45°C on (a) PiPAC-MB and (b) PoPAC-MB	155
Figure B2	MB percent removal versus adsorption time at various initial concentrations at 45°C on (a) PiPAC-MB and (b) PoPAC-MB	155
Figure B3	MB adsorption uptake versus adsorption time at various initial concentrations at 60°C on (a) PiPAC-MB and (b) PoPAC-MB	156
Figure B4	MB percent removal versus adsorption time at various initial concentrations at 60°C on (a) PiPAC-MB and (b) PoPAC-MB	156
Figure B5	MR adsorption uptake versus adsorption time at various initial concentrations at 45°C on (a) PiPAC-MR and (b) PoPAC-MR	157
Figure B6	MR percent removal versus adsorption time at various initial concentrations at 45 °C on (a) PiPAC-MR and (b) PoPAC-MR	157
Figure B7	MR adsorption uptake versus adsorption time at various initial concentrations at 60°C on (a) PiPAC-MR and (b) PoPAC-MR	158
Figure B8	MR percent removal versus adsorption time at various initial concentrations at 60 °C on (a) PiPAC-MR and (b) PoPAC-MR	158
Figure B9	RBV adsorption uptake versus adsorption time at various initial concentrations at 45 °C on (a) PiPAC-RBV and (b) PoPAC-RBV	159
Figure B10	RBV percent removal versus adsorption time at various initial concentrations at 45 °C on (a) PiPAC-RBV and (b) PoPAC-RBV	159

Figure B11	RBV adsorption uptake versus adsorption time at various initial concentrations at 60 °C on (a) PiPAC-RBV and (b) PoPAC-RBV	160
Figure B12	RBV percent removal versus adsorption time at various initial concentrations at 60 °C on (a) PiPAC-RBV and (b) PoPAC-RBV	160
Figure C1	Graph of adsorption isotherm models for PiPAC-MB at temperature 45°C	161
Figure C2	Graph of adsorption isotherm models for PiPAC-MB at temperature 60°C	161
Figure C3	Graph of adsorption isotherm models for PoPAC-MB at temperature 45°C	162
Figure C4	Graph of adsorption isotherm models for PoPAC-MB at temperature 60°C	162
Figure C5	Graph of adsorption isotherm models for PiPAC-MR at temperature 45°C	165
Figure C6	Graph of adsorption isotherm models for PiPAC-MR at temperature 60°C	165
Figure C7	Graph of adsorption isotherm models for PoPAC-MR at temperature 45°C	166
Figure C8	Graph of adsorption isotherm models for PoPAC-MR at temperature 60°C	166
Figure C9	Graph of adsorption isotherm models for PiPAC-RBV at temperature 45°C	169
Figure C10	Graph of adsorption isotherm models for PiPAC-RBV at temperature 60°C	169
Figure C11	Graph of adsorption isotherm models for PoPAC-RBV at temperature 45°C	170
Figure C12	Graph of adsorption isotherm models for PoPAC-RBV at temperature 60°C	170
Figure D1	Plots of separation factor versus MB initial concentration for adsorption of PiPAC-MB and PoPAC-MB at 45°C	173
Figure D2	Plots of separation factor versus MB initial concentration for adsorption of PiPAC-MB and PoPAC-MB at 60°C	173
Figure D3	Plots of separation factor versus MR initial concentration for adsorption of PiPAC-MR and PoPAC-MR at 45°C	174

Figure D4	Plots of separation factor versus MR initial concentration for adsorption of PiPAC-MR and PoPAC-MR at 60°C	174
Figure D5	Plots of separation factor versus RBV initial concentration for adsorption of PiPAC-RBV and PoPAC-RBV at 45°C	175
Figure D6	Plots of separation factor versus RBV initial concentration for adsorption of PiPAC-RBV and PoPAC-RBV at 60°C	175
Figure G1	Boyd plots for adsorption of MB onto (a) PiPAC-MB and (b) PoPAC-MB at 45°C	174
Figure G2	Boyd plots for adsorption of MB onto (a) PiPAC-MB and (b) PoPAC-MB at 60°C	194
Figure G3	Boyd plots for adsorption of MR onto (a) PiPAC-MR and (b) PoPAC-MR at 45°C	195
Figure G4	Boyd plots for adsorption of MR onto (a) PiPAC-MR and (b) PoPAC-MR at 60°C	195
Figure G5	Boyd plots for adsorption of RBV onto (a) PiPAC-RBV and (b) PoPAC-RBV at 45°C	196
Figure G6	Boyd plots for adsorption of RBV onto (a) PiPAC-RBV and (b) PoPAC-RBV at 60°C	196

LIST OF PLATES

Plate 1.1	Precursors; (a) pineapple peel and (b) pomelo peel	3
Plate 2.1	Precursors; (a) pineapple fruit and (b) pomelo fruit	13
Plate 2.2	Scanning electron micrographs; (a) MP; (b) MP char; and (c) MP activated carbon (magnifications: 500x)	21
Plate 4.1	SEM micrographs of (a) PiP (magnification: 1200x); and (b) PiPAC (magnification: 80000x)	79
Plate 4.2	SEM micrographs of (a) PoP (magnification: 1200x); and (b) PoPAC (magnification: 50000x)	79

LIST OF SYMBOLS

		Unit
A	Arrhenius factor	-
A_i	Measured absorbance for component i	-
A_T	Constant for Temkin isotherm	L/g
A_{KC}	Constant for Koble-Corrigan isotherm	$L^n \text{mg}^{1-n}/\text{g}$
b_c	path length of the cell	-
b_T	Constant for Temkin isotherm	mg/g h
b_{To}	Constant for Toth isotherm	L/mg
B_i	Constant for Boyd model	-
B_{KC}	Constant for Koble-Corrigan isotherm	L/mg ⁿ
C	Solute/outlet concentration	mg/L
C_e	Concentration of adsorbate at equilibrium	mg/L
C_i	Constant for Intraparticle diffusion model	mg/g
C_t	Concentration of adsorbate at time, t	mg/L
C_o	Initial/inlet adsorbate concentration	mg/L
D_p	Average pore diameter	nm
E_a	Arrhenius activation energy of adsorption	kJ/mol
F	Fraction of solute adsorbed for Boyd model	-
K_F	Adsorption or distribution coefficient for Freundlich isotherm	$\text{mg/g} (\text{L/mg})^{1/n}$
K_L	Rate of adsorption for Langmuir isotherm	L/mg
k_{Av}	Avrami kinetic constant	-
k_{pi}	Adsorption rate constant for intraparticle diffusion model	$\text{mg/g h}^{1/2}$
k_1	Adsorption rate constant for pseudo-first-order	1/h
k_2	Adsorption rate constant for pseudo-second-order	g/mg h
k_s	Sips isotherm model constant	L/mg
K_{BS}	Brouwers Sotolongo constant	-
K_{RP}	Radke-Praschnitz model constant	-
k_{VS}	Vieth-Sladek constant	-
m_{RP}	Radke-Praschnitz model exponent	-
m_s	Sips isotherm model exponent	-

N	Total number of experiments required/data point	-
n_{Av}	Avrami kinetic constant	-
n_F	Constant for Freundlich isotherm	-
n_{KC}	Adsorption intensity Koble-Corrigan isotherm	-
n_{To}	Toth constant	mg/g
Q_o	Adsorption capacity for Langmuir isotherm	mg/g
Q_m	Maximum adsorption capacity of adsorbent	mg/g
q_e	Amount of adsorbate adsorbed per unit mass of adsorbent at equilibrium	mg/g
q_t	Amount of adsorbate adsorbed per unit mass of adsorbent at time, t	mg/g
$q_{t, cal}$	Calculated adsorption uptake at time, t	mg/g
$q_{t, exp}$	Experimental adsorption uptake at time, t	mg/g
R	Universal gas constant	8.314 J/mol K
R_L	Separation factor	-
R^2	Correlation coefficient	-
S_{BET}	BET surface area	m ² /g
T	Absolute temperature	K
T	Time	h
V	volume of the solution	L
V_{meso}	Mesopore volume	cm ³ /g
V_T	Total pore volume	cm ³ /g
W	mass of adsorbent	g
w_c	Dry weight of prepared activated carbon	g
w_o	Dry weight of precursor	g
$w_{Na_2CO_3}$	Dry weight of sodium carbonate	g
X	Activated carbon preparation variable	-
Y	Predicted response	-
<i>Greek letters</i>		
ΔG°	Changes in standard free energy	kJ/mol
ΔH°	Changes in standard enthalpy	kJ/mol
Δq_t	Normalized standard deviation	%
ΔS°	Changes in standard entropy	J/mol K

α_{BS}	Brouoers-Sotolongo constant	-
α_{EI}	initial desorption rate for Elovich kinetic model	mg/(g min)
α_t	adsorption fraction of time of Avrami kinetic model	-
λ	Wavelength	nm
ε_λ	molar absorptivity coefficient of solute at wavelength	-
β_{EI}	desorption constant for Elovich kinetic model	g/mg
β_{VS}	Vieth-Sladek constant	-
λ	Wavelength	nm

LIST OF ABBREVIATIONS

AC	Activated carbon
ANOVA	Analysis of variance
BET	Brunauer-Emmett-Teller
CCD	Central composite design
FTIR	Fourier Transform Infrared
IR	Impregnation ratio
IUPAC	International Union of Pure and Applied Chemistry
MB	Methylene blue
MP	Mangosteen peel
MR	Methyl red
MSDS	Material Safety Data Sheet
PiPAC	Pineapple peel activated carbon
PoPAC	Pomelo peel activated carbon
RBV	Remazol brilliant violet 5R
RSM	Response surface methodology
SEM	Scanning electron microscopy
STA	Simultaneous thermogravimetric analyser

PENYEDIAAN KARBON TERAKTIF DARIPADA KULIT NENAS DAN KULIT LIMAU BALI UNTUK PENYINGKIRAN PEWARNA: KAJIAN KESEIMBANGAN, KINETIK DAN TERMODINAMIK

ABSTRAK

Kajian penghasilan karbon teraktif daripada kulit nenas (KTKN) dan kulit limau bali (KTKL) melalui pengaktifan fizi-kimia yang terdiri daripada jerap isi kalium hidroksida (KOH) dan gasifikasi karbon dioksida (CO₂) telah berjaya dilaksanakan. Karbon teraktif yang terhasil telah digunakan untuk penyingkiran pewarna metilina biru (MB), metil merah (MM) dan remazol brilliant ungu 5R (RBU) daripada larutan akuas. Keputusan rekabentuk ujikaji telah menunjukkan bahawa suhu pengaktifan, masa pangaktifan dan nisbah jerap isi merupakan faktor-faktor penting yang mempengaruhi prestasi penjerapan pewarna MB, MM dan RBU. Keadaan optimum untuk penyediaan KTKN dan KTKL untuk penyingkiran MB adalah pada suhu pengaktifan, masa pengaktifan dan nisbah jerap isi masing-masing pada 732°C, 1.96 jam, 3.00, dan 750°C, 2.19 jam, 2.12. Manakala keadaan optimum untuk penyediaan KTKN dan KTKL untuk penyingkiran MM adalah pada suhu pengaktifan, masa pengaktifan dan nisbah jerap isi masing-masing pada 748°C, 2.13 jam, 3.00, dan 800°C, 2.19 jam, 2.96. Manakala untuk penyingkiran RBU, keadaan optimum untuk penyediaan KTKN dan KTKL adalah masing-masing pada suhu pengaktifan, masa pengaktifan dan nisbah jerap isi 737°C, 2.50 jam, 1.41, dan 763°C, 1.20 jam, 3.19. Kesemua karbon teraktif yang terhasil adalah berliang meso dengan luas permukaan yang tinggi. Morfologi karbon teraktif yang terhasil memaparkan struktur liang yang heterogen. Terdapat pelbagai kumpulan berfungsi pada permukaan karbon teraktif. Kesan daripada kepekatan awal pewarna (25-300 mg/L), masa sentuh (0-24 jam), suhu larutan (30-60°C), dan pH larutan (2-12) telah

dinilai melalui kajian penjerapan berkelompok. Penjerapan semua pewarna meningkat dengan meningkatnya kepekatan awal larutan dan masa sentuh. Penjerapan pewarna MB oleh KTKN-MB adalah sesuai dipadankan oleh model garis sesuhu *Freundlich*, *Toth* dan *Brouers-Sotolongo*, manakala untuk KTKL-MB adalah sesuai diterangkan oleh model *Freundlich* dan *Toth*. Penjerapan MM oleh KTKN-MM adalah masing-masing sesuai dihuraikan oleh model *Temkin* dan *Vieth-Sladek*, manakala KTKL-MM ialah model *Vieth-Sladek*. Penjerapan RBU oleh KTKN-RBU adalah sesuai dipadankan oleh model garis sesuhu *Langmuir*, *Koble-Corrigan*, *Sips* dan *Toth*, manakala KTKL-RBU sesuai dipadankan oleh model *Langmuir*, *Temkin* dan *Toth*. Penjerapan MB oleh KTKN-MB dan KTKL-MB terbaik dipadankan oleh model kinetik pseudo tertib kedua. Untuk penjerapan MM oleh KTKN-MM dan KTKL-MR sesuai dihuraikan oleh model kinetik pseudo tertib pertama. Manakala, penjerapan RBU oleh KTKN-RBU dan KTKL-RBU masing-masing sesuai dipadankan oleh model kinetik pseudo tertib kedua dan model kinetik pseudo tertib pertama. Kesemua proses penjerapan adalah ditadbir oleh mekanisme kawalan-serapan-filem. Kesemua proses penjerapan yang dikaji menunjukkan tenaga pengaktifan yang lebih rendah dari 46.12 kJ/mol yang mencirikan mekanisme penjerapan secara jerapan fizikal.

PREPARATION OF ACTIVATED CARBON FROM PINEAPPLE PEEL AND POMELO PEEL FOR DYES REMOVAL: EQUILIBRIUM, KINETIC AND THERMODYNAMIC STUDIES

ABSTRACT

The production of activated carbon from pineapple peel (PiPAC) and pomelo peel (PoPAC) through physiochemical activation consisting of potassium hydroxide (KOH) impregnation and carbon dioxide (CO₂) gasification has been successfully investigated. Activated carbon produced were used for removal of methylene blue (MB), methyl red (MR) and remazol brilliant violet 5R (RBV) dyes from aqueous solution. The experimental design results revealed that the activation temperature, activation time and KOH impregnation ratio (IR) were significant factors influencing adsorption performance for MB, MR and RBV. The optimum preparation conditions of PiPAC and PoPAC for MB removal were at activation temperature, activation time and IR of 732°C, 1.96 hour, 3.00, and 750°C, 2.19 hour, 2.12, respectively. Whereas optimum preparation conditions obtained for PiPAC and PoPAC for MR removal were at activation temperature, activation time and IR of 748°C, 2.13 hour, 3.00, and 800°C, 2.19 hour, 2.96, respectively. While for RBV removal, the optimum preparation conditions of PiPAC and PoPAC were at activation temperature, activation time and IR of 737°C, 2.50 hour, 1.41, and 763°C, 1.20 hour, 3.19, respectively. All the activated carbons prepared were mesoporous with high surface area. The prepared activated carbons were demonstrated heterogeneous type of pore structures. There were presences of various functional groups on the activated carbon surfaces. The effects of adsorbate initial concentration (25-300 mg/L), contact time (0-24 h), solution temperature (30-60°C), and solution pH (2-12) were evaluated through batch adsorption test. All dyes adsorption uptakes increased with increasing

initial concentration and contact time. Adsorption of MB dye onto PiPAC-MB were best fitted by Freundlich, Toth and Brouers-Sotolongo models, whereas for PoPAC-MB were best described by Freundlich and Toth models. Adsorptions of MR onto PiPAC-MR were better fitted by the Temkin and Vieth-Sladek model while for PoPAC-MR was Vieth-Sladek model, respectively. On the other hand, adsorption of RBV onto PiPAC-RBV was well fitted by Langmuir, Koble-Corrigan, Sips and Toth isotherm model, whereas for PoPAC-RBV was best described by Langmuir, Temkin and Toth models, respectively. Adsorptions of MB onto PiPAC-MB and PoPAC-MB were best fitted by pseudo-second-order kinetic model. For MR adsorption onto PiPAC-MR and PoPAC-MR demonstrates applicability of pseudo-first-order kinetic model, respectively. On the other hand, RBV adsorption onto PiPAC and PoPAC were well fitted by pseudo-second-order and pseudo-first-order kinetic model, respectively. All the adsorption processes were mainly governed by the film-diffusion-controlled mechanism. All the adsorption processes investigated show activation energy values lower than 46.12 kJ/mol which representing physisorption mechanism.

CHAPTER ONE

INTRODUCTION

1.1 Dyes in textile industries

Dyes have been extensively used in textile industries. Dyes can be classified according to their type, which reflect their macroscopic behavior and their application. There are various type of dyes used in textile industries such as acid dyes, basic dyes, disperse dyes, direct dyes, reactive dyes, solvent dyes, sulfur dyes and vat dyes. The most common dyes used in textile industries are basic dye, reactive dye and acid dye. Basic dye, such as methylene blue (MB), has chromophore with positive ion and amino groups with high color intensity (Rafatullah, *et al.*, 2010). MB is commonly used for dyeing cotton and silk. However, MB is difficult to be degraded or removed from aqueous solution due to its stability to heat, light and oxidizing agents (Robinson *et al.*, 2001). MB can cause injury to eyes of human and animal. On inhalation, it may cause short periods of difficulty in breathing, while ingestion in mouth can cause nausea, vomiting, profuse sweating and mental confusion (Tan *et al.*, 2008a).

Almost 45% of textile produced worldwide belongs to the reactive dyes (Tunc *et al.*, 2009). They have the favorable characteristics of bright color, simple application techniques, low energy consumption dyeing process and high solubility in water. Reactive dyes are typically azo-based chromophores combined with different types of reactive groups. They bind to the textile fibers such as cotton to form covalent bonds. Example of reactive dyes are remazol brilliant blue R (RBBR), remazol black (RB) and remazol brilliant violet 5R (RBV). The usages of reactive dyes are highly carcinogenic and possess toxic to some organism (Papic *et al.*, 2004).

Acid dye is soluble in water, anionic compounds and commonly used on wool and nylon. Acid dye is characterized by the presence of $-N=N-$ bond (Igwe, 2007). Acid dye such as methyl red (MR) and methyl orange (MO) can cause irritation of the eye, skin and digestive tract if inhaled or swallowed (Badr *et al.*, 2008).

Overall, dyes are considered as pollutant in aquatic environment since they can cause undesirable color to the water, reduce light penetration and prevent photosynthesis. The discharge of untreated textile effluent can cause natural waters to be unfit as potable water source. It is well known that 70-80% of all illness in developing country is related to water contamination (WHO, 2000). Therefore, the removal of dyes from industrial effluent is important before discharging it into receiving water bodies. Various methods of dyes removal exist, but adsorption on activated carbons derived from agricultural wastes appears to be efficient and cheaper to purify polluted water.

1.2 Agricultural waste based adsorbent

Adsorption process is known to be very practical for dyes wastewater treatment provided the adsorbent used is cheap. The growing of interest to find cheaper and renewable sources for activated carbon particularly from agricultural wastes is increasing recently. Agricultural wastes are defined as wastes produced from agro-based industries which have no commercial value and commonly been dumped on the site. Agriculture wastes such as coconut husk (Tan *et al.*, 2008a), rice husk (Kalderis *et al.*, 2008), mangosteen peel (Ahmad and Alrozi, 2010), jackfruit peel (Prahas *et al.*, 2008), cherry stones (Jaramillo *et al.*, 2009), peanut hull (Tanyildzi, 2011) and waste tea (Auta and Hameed, 2011) have been proved suitable

as precursors for production of activated carbon. Utilization of these wastes prevents on-site burning and saves on disposal cost.

Pineapple (*Ananas Cosmosus*) industry plays an important role in the country's socio-economic development of Malaysia, particularly in Johor. Pineapple is traded in form of canned pineapple, pineapple concentrate and fresh fruit. Canned pineapple is grouped into slices, crushed, chunks and cube. The pineapple juice can be consumed as a straight or mixed with other juices. According to Lembaga Perindustrian Nanas Malaysia (LPNM), production of pineapple in Malaysia was 600 metric tons for 2011. Large production of pineapple-based-product indicates large production of peel as waste (Plate 1.1(a)) which is estimated as 10% of total weight of pineapple fruit. It has a potential to be used as precursor for activated carbon since pineapple peel is material rich in lignocellulosic component.

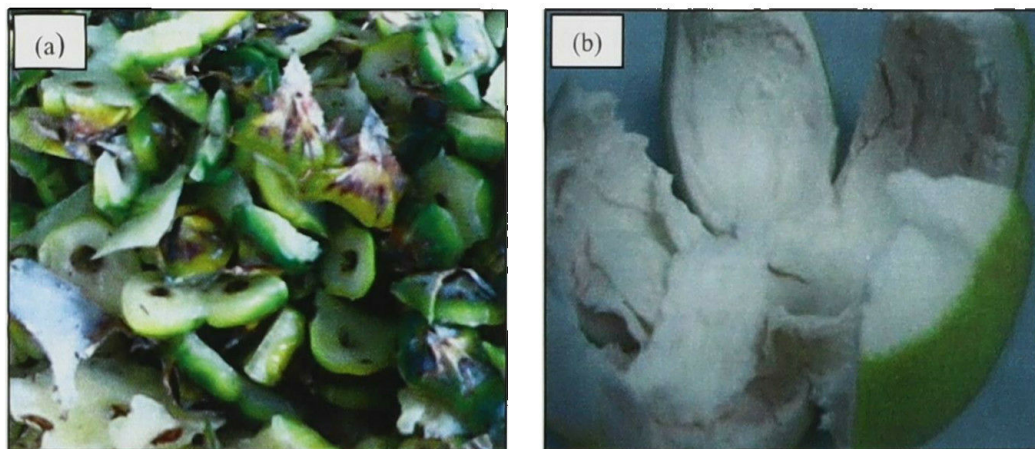


Plate 1.1 Precursors; (a) pineapple peel and (b) pomelo peel

Pomelo (*citrus grandis*) is a crisp citrus fruit native to Southeast Asia. The outer skin is rough and dark green-colored. The inner skin is spongy-like and white in color. In Malaysia, approximately 1895 hectares of pomelo trees are grown commercially, with an estimated annual production of 8830 metric tons of pomelo

fruits (Foo and Hameed, 2011). The pomelo plantations are abundantly available in Johor and Perak. The pomelo can be consumed as jam, salad and curd. However, the peel (Plate 1.1 (b)) is bitter and always discarded as waste. Therefore, in this work pineapple peel (PiP) and pomelo peel (PoP) were utilized for activated carbon production.

1.3 Problem statement

The discharges of large amount of dyes from textile industry raise an environmental concern due to their high visibility and toxicity. The common dyes in industry are basic dye, acid dye and reactive dye groups. These dyes affect reflection of sunlight penetrated into water and interferes growth of aquatic organism. The complex structure and high solubility of dyes in water cause them difficult to be removed from wastewater.

The adsorption process is found suitable for dyes removal particularly if the adsorbent used is from cheap and renewable material. Current commercial coal-based adsorbent is prepared from non-renewable and expensive precursor. Therefore, in this work, pineapple peel (PiP) and pomelo peel (PoP) are utilized as raw materials for activated carbon production. It is an added advantage to the agricultural waste industry if the excess of PiP and PoP can be turned into useful and valuable adsorbent. The activated carbons prepared were used to remove basic, acid and reactive dyes from aqueous solution.

1.4 Scope of study

Adsorption has been found to be an efficient and economically cheap process for removing dyes using various adsorbents (Kavitha and Namasivayam 2007). The

use of activated carbons has been widely favored because of their high adsorption capacities and amphoteric properties which enable their adsorption of both cationic and anionic effluents (Al-Degs *et al.*, 2000). Accordingly, research has been devoted towards the utilization of agricultural waste available from fields or generated from the industrial manufacturing plants (Foo and Hameed, 2011). In this work, the pineapple peel and pomelo peel were utilized to prepare activated carbon for MB, MR and RBV dyes removal. The preparation of activated carbon was done using physiochemical method which applies impregnation of KOH to improve adsorptive characteristic of activated carbon.

The optimizations of the operating parameters are including activation temperature, activation time and IR were done using response surface methodology method (RSM). RSM will generate the design of experiment and the response for every experimental run will be analyzed to obtain optimum operating condition for preparation of PiPAC and PoPAC for dyes removal as well as activated carbon yield.

The optimized activated carbon were latter characterized in terms of surface area, surface morphology, proximate content and surface chemistry by using SEM, STA and FTIR, respectively. The precursor and char samples were also included for comparison purpose.

The optimized PiPAC and PoPAC were then used in equilibrium, kinetic and thermodynamic studies to investigate the adsorption behavior of each dye (MB, MR and RBV) onto activated carbons. In order to carry out the analysis, batch adsorption study were done by examine the effect of adsorbate initial concentration (25-300 mg/L), contact time (0-24 hour), solution temperature (30-60°C) and solution pH (2-12) for adsorption of dyes onto activated carbons prepared.

1.5 Research objectives

This research aims,

- i) To prepare pineapple peel based activated carbon (PiPAC) and pomelo peel based activated carbon (PoPAC) using physiochemical activation.
- ii) To optimize the operating parameters in the preparation of PiPAC and PoPAC using response surface methodology.
- iii) To characterize PiPAC and PoPAC in terms of surface area, surface morphology, proximate content and surface chemistry.
- iv) To study the effects of adsorbate initial concentration, contact time, solution temperature and solution pH for adsorption of methylene blue (MB), methyl red (MR) and remazol brilliant violet 5R (RBV) on PiPAC and PoPAC for equilibrium, kinetic and thermodynamic studies.

1.6 Organization of thesis

The thesis consists of five chapters, where each chapter represents an important build for general construction of the thesis. Chapter one presents research background, problem statement and objectives of the work. Chapter two presents a literature review which covered the dyes wastewater treatment, utilization of agricultural waste in activated carbon production and dye removal studies. In addition, an overview of various precursors and activation method have been used to prepare activated carbons are provided in this chapter. Information on optimization of activated carbon preparation condition is discussed. The last section consists of the adsorption isotherm, kinetics and thermodynamic for batch adsorption system.

Chapter three presents list of materials and chemicals reagents used in the research work. The experimental procedures are consisting of precursor preparation,

experimental design for the activated carbon preparation, model fitting and statistical analysis. Batch equilibrium, kinetic and thermodynamic studies are then explained. It is followed by the schematic flow diagram showing the overall activities carried out in this research.

Chapter four is divided into three main sections. The first section presents the developed regression model, together with the optimization results based on the percentage dyes removal and activated carbon yield. Section two discusses on the characterization of the PiPAC and PoPAC. Section three covers the batch adsorption studies of dyes on activated carbon prepared.

Chapter five finally presents the conclusions that reflect the achievements of all the objectives which were obtained throughout the study as well as the recommendations for the future research. These recommendations offered the significance and importance related to the present research.

CHAPTER TWO

LITERATURE REVIEW

2.1 Dyes wastewater treatment

Color is the first contaminant to be recognized in textile wastewater. The presence of even very small amounts of dyes in water is highly visible and undesirable. Wastewater treatment process selection is a complex task involving the consideration of many factors which include; available space for the construction of treatment facilities, reliability of process equipment, waste disposal constraint, desired finished water quality and capital cost as well as operating cost (Bhatnagar and Silaanpar, 2010).

During the past three decades, several physical, chemical and biological decolorization methods have been reported (Rafatullah *et al.*, 2010). A number of technologies are available with varying degree of success to control water pollution were summarized by Crini (2006) with their respective advantages and disadvantages, as listed in Table 2.1. All these methods have different color removal capabilities, capital cost and operating rates (Amin, 2009). These methods also suffer from one or other limitations, and none of them were successful in completely removing the color from wastewater (Sulak *et al.*, 2007). However, at the present time, there is no single process capable of adequate treatment, mainly due to the complex nature of the textile effluents (Tan *et al.*, 2008a).

Table 2.1 Principal existing and emerging processes for dyes removal (Crini, 2006)

Technology		Advantages	Disadvantages
Conventional treatment processes	Coagulation and flocculation	Simple, economically feasible	High sludge production, handling and disposal problems
	Biodegradation	Economically attractive, publicly acceptable treatment	Slow process, necessary to create an optimal favorable environment, maintenance and nutrition requirements.
	Adsorption on activated carbons	The most effective adsorbent, great, capacity, produce a high-quality treated effluent	Ineffective against disperse and vat dyes, the regeneration is expensive and results in loss of the adsorbent, non-destructive process
Established recovery processes	Membrane separations	Removes all dye types, produce a high-quality treated effluent	High pressure, expensive, incapable of treating large volumes
	Ion-exchange	No loss of sorbent on regeneration, effective	Economic constraints, not effective for disperse dyes
	Oxidation	Rapid and efficient process	High energy cost, chemicals required
Emerging removal processes	Advanced oxidation process	No sludge production, little or no consumption of chemicals, efficiency for recalcitrant dyes	Economically unfeasible, formation of by-products, technical constraints
	Selective bioadsorbents	Economically attractive, regeneration is not necessary, high selectivity	Requires chemical modification, non-destructive process
	Biomass	Low operating cost, good efficiency and selectivity, no toxic effect on microorganisms	Slow process, performance depends on some external factors (pH, salts)

Adsorption technique has many advantages over several other methods for wastewater treatment. It needs less land area as compared to biological system, not getting affected by toxic chemicals and superior removal of organic contaminants. Furthermore, design flexibility, ease of operation and does not result in formation of harmful substance were among advantages of adsorption technique (Rafatullah *et al.*,

2009). By referring to the abundant literature data, liquid-phase adsorption is one of the most popular methods for the removal of pollutants from wastewater since proper design of the adsorption process will produce a high-quality treated effluent (Crini, 2006). Currently, commercial coal-based activated carbon is commonly used as adsorbent; however, its widespread use is restricted due to its relatively high cost which led to the researches on alternative renewable and low-cost adsorbents.

Dye adsorption is a process of transfer of a dye molecule from bulk solution phase to the interface. The adsorption process occurs as resulted from interactions between the adsorbent surface and the adsorbate. There are numerous factors that affect the dye adsorption, including interaction between adsorbate and adsorbent, adsorbent surface area, adsorbent pore structure, adsorbent surface chemistry, characteristics of dye molecule, solution pH, temperature and contact time (Mezohegyi *et al.*, 2012). As various factor affects adsorption efficiency, thus the adsorption behaviors study for each type of adsorbent and adsorbate are equally important. In literature, activated carbon adsorbent has been found suitable to remove metal ion, anions, dyes, phenols, detergents, pesticides and chlorinated hydrocarbons from aqueous solution.

2.2 Activated carbon precursor

Adsorption methods employing solid sorbents are widely used to remove certain classes of chemical pollutants from wastewater. However, amongst all the sorbent materials proposed, activated carbon is the most popular for the removal of pollutants from wastewater (Demirbas *et al.*, 2009). Activated carbon has been preferred as an adsorbent for dyes wastewater treatment, however, commercial activated carbons are considered expensive due to the utilization of non-renewable

and expensive starting materials such as coal (Tan *et al.*, 2008a). Table 2.2 below shows the adsorption capacities for various activated carbons derived from agricultural wastes for adsorption of methylene blue dyes. The adsorption capacity of activated carbon depends not only on its surface area, but also on its internal pore structure, surface characteristic and the presence of functional group on pore surface. Internal pore structure and surface characteristic play an important role in adsorption processes and depends both on the precursor used and method of preparation (Ismadji *et al.*, 2005).

Table 2.2 Adsorption capacities for activated carbons derived from agricultural wastes

Activated carbon precursor	Adsorption capacity (mg/g)	Reference
Tea wood bark	914.59	(McKay <i>et al.</i> , 2009)
Papaya seeds	555.55	(Hameed, 2009a)
Rice husk	312.26	(McKay <i>et al.</i> , 2009)
Jackfruit peel	285.71	(Hameed, 2009b)
Banana stalk waste	243.90	(Hameed <i>et al.</i> , 2008)
Cedar sawdust	142.36	(Hamdoui, 2006)
Meranti sawdust	120.48	(Ahmad <i>et al.</i> , 2009)
Pineapple stem	119.05	(Hameed <i>et al.</i> , 2009)
Garlic peel	82.64	(Hameed and Ahmad, 2009)
Ground hazelnut shell	76.90	(Ferrero, 2009)
Peanut hull	68.03	(Gong <i>et al.</i> , 2005)
Coffee husk	90.10	(Oliveira <i>et al.</i> , 2008)
Cherry sawdust	39.84	(Ferrero, 2009)
Olive pomace	42.3	(Banat <i>et al.</i> , 2007)
Oak sawdust	29.94	(Ferrero, 2009)
Banana peel	20.80	(Annadurai <i>et al.</i> , 2002)
Orange peel	18.60	(Annadurai <i>et al.</i> , 2002)
Wheat shells	16.56	(Bulut and Aydin, 2006)

Water treatment provides both the largest market and the main area of growth for activated carbons in fact it is known that around 80% of the world production of activated carbons is used in liquid phase applications (Dias *et al.*, 2007; Gaur and

Shankar, 2008). Therefore, the development of activated carbon from low cost and renewable precursors, which can be used more economically on large scale, is equally important. Agricultural wastes have been shown to have potential as precursor materials in the preparation of activated carbons, which are available freely and abundantly. It can be prepared from a wide variety of raw materials, having high organic (carbon) content and low inorganic content and these can be easily activated (Castilla and Utrilla, 2001).

2.2.1 Pineapple (*Ananas comosus L.*) peel

Pineapple (Plate 2.1 (a)) is an herbaceous perennial plant with a height of 1.0-1.5 m and pointed leaves surrounding thick stem, are abundantly available in Malaysia. It is a composite of many flowers whose fruitlets fuse together around a central core. Pineapple has wide cylindrical shape, scaly green, yellow skin and also regal crown of spiny. It has blue green leaves and fibrous yellow flesh (Medina and Garcia, 2005). Typically, pineapple took 18 months to grow. Pineapple tastes sweet and delicious, thus, suitable eaten fresh, canned or juice. Apart being consumed in food manufacturing, it also been used in pharmaceutical industries (Ketnawa *et al.*, 2012).

Its wide scale cultivation and implementation by the food manufacturing industries are deteriorated by the massive generation of peel and stem waste (Foo and Hameed, 2012). The waste portions such as the peel, core, stem and crown were 29-40%, 9-10%, 2-5% and 2-4% (w/w), respectively (Ketnawa *et al.*, 2012). Therefore, the utilization of pineapple peel would be advantage in saving disposal cost and able to become precursor of activated carbon.

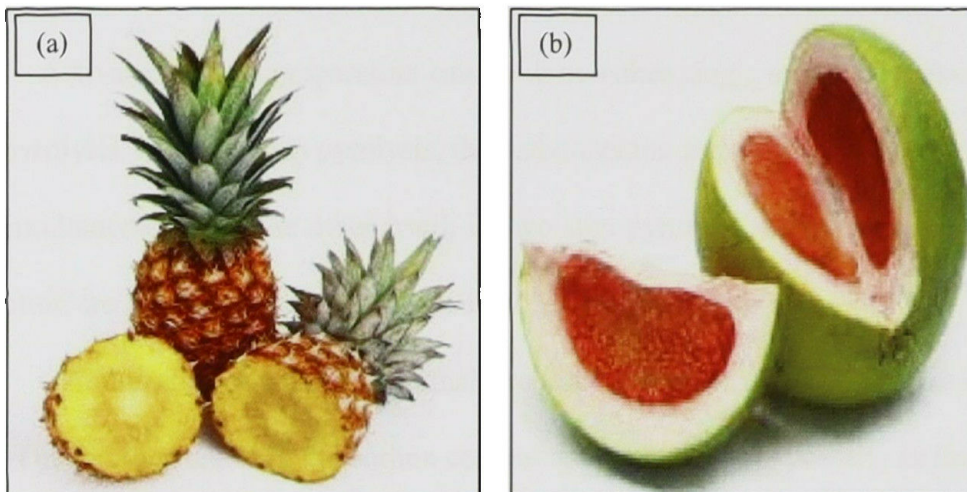


Plate 2.1 Precursor; (a) pineapple and (b) pomelo fruit

2.2.2 Pomelo (*Citrus grandis L.*) peel

Pomelo (Plate 2.1 (b)) is known to be 'king of the citrus fruit kingdom' for its size. It does vary in color, from dark green to yellow. It has very thick skin up to 2 inches. The inner skins are spongy-like and white in color. The inner fruit ranges in color from white to pink. Pomelo produces fruit throughout the year with peak season between January and February and August to September (Hien and Tung, 2006). Pomelo are usually eaten fresh, and available as food supplement in deserts, salads, fruit cocktail, jam, juice combination or food processing industries (Foo and Hameed, 2011). Additionally, pomelo has been utilized in cosmetic and pharmaceutical (Hien and Tung, 2006). However, peels, seeds and fruit pulps, which account for 50% of the original whole fruit mass, are often considered inedible and discarded. Thus, utilization of pomelo peel for productions of activated carbon is able to enhance value of pomelo waste and saves on disposal cost.

2.3 Preparation method of activated carbon from agricultural waste

Activated carbon preparation can be done either single step pyrolysis or two step pyrolysis. In single step pyrolysis, the carbonization and activation step are carry out simultaneously. On the other hand, in two step pyrolysis, the carbonization and activation are done separately (Ioannidou and Zabaniotou, 2007).

Carbonization is an inert thermal process to convert raw material into solid char. This process enriches the carbon content and creates initial porosity in the char. The carbonization temperature commonly ranges between 400 to 850°C. During the carbonization process, components in agricultural waste (hemicelluloses, cellulose and lignin) would undergo dehydration reaction and linkage breaking to form solid char (Li *et al.*, 2008).

Activation is a sequence process to enhance the char porosity and clean out the tar clogging pores (Turmuzi *et al.*, 2004). Activation of char can be done either physically, chemically or combination of physical and chemical method. In physical activation, the char is pyrolyzed at elevated temperature in the presence of suitable oxidizing gas such as carbon dioxide (CO₂), oxygen (O₂) and steam. CO₂ is usually used as it is clean and easy to handle (Zhang *et al.*, 2004). The reaction between carbon atom and the oxidizing gas gives rise to the pore creation and enlarge the existing pores.

Chemical activation carried out with char being impregnated with chemical activating agents such as ZnCl₂, KOH, H₃PO₄, K₂CO₃ and NaCO₃ (Ioannidou and Zabaniotou, 2007). Chemical activation has advantages over physical activation as it can be performed at lower temperatures and shorter times. The impregnation ratio (IR) is calculated by the weight ratio of the char sample to the chemical used. Optimum IR is important to create well developed pore on the adsorbent's surface. It

led to the formation of large surface area and high adsorption capacity. KOH is an effective activating agent due to its selectiveness in activation process (Rodenas *et al.*, 2007). General chemical reaction between KOH and carbon material are as follows (Viswanathan *et al.*, 2009):



However at higher IR, the chemical will form insulating layers which cover and block the pores (Girgis and El-Hendawy, 2002). Mopoung (2008) found that at very high IR of KOH, white spheres and fluffy materials were appeared due to the presence of K_2O and K_2CO_3 or K residues in pore surface of char. Hence, optimum IR needs to be identified in order to achieve desirable activated carbon characteristics.

Physiochemical activation consists of both physical and chemical treatment. The sample was first impregnated with chemical agent similar as chemical activation technique, before undergo CO_2 activation to produce activated carbon. This chemical influences the pyrolytic decomposition and retard the tars formation during the activation process. The presence of chemical raises the pore size and porosity of activated carbon in addition to CO_2 gasification (Mopoung, 2008). The combination of chemical and physical treatment has potential to improve pore development at lower activation temperature due to the effect of chemicals (Diao *et al.*, 2002). Therefore, it will reduce the consumption of energy by aids of chemical treatment for production of activated carbon.

2.4 Influence of preparation variable to activated carbon

Characteristics of activated carbon produced commonly vary based on the nature of raw materials and activation process (Chandra *et al.*, 2009). Activation

temperature, activation time, and IR are preparation variables that found to have great influence towards activated carbon properties (Tan *et al.*, 2008b).

The activation process for activated carbon preparation required the presence of suitable oxidizing agent such as CO₂. CO₂ is clean, easy to handle and it facilitates control of the activation process due to the slow reaction rate (Zhang *et al.*, 2004). In recent study by Guo *et al.* (2009) reported the significant effect of CO₂ activation on porous structures of coconut shell-based activated carbons. It was found that the yield and average pore diameter of activated carbons decreased; while the BET surface area, micropore volume; total pore volume increased with increasing activation temperature from 750 to 900°C due to a combination of releasing of volatiles and weak oxidation of char with carbon dioxide.

Activation temperature causes CO₂ and surface metal complex to further gasify the carbon, which leads to pore widening (Tseng *et al.*, 2006). The reaction rate between carbon and chemical impregnate increased with increased in activation temperature, thus, enhanced the existing pore and creates new porosity. The development of pore to the desirable pore size is important in improving adsorption capacity. For instance, small pore size will not trap large adsorbate molecules and large pores may not be able to retain small adsorbates, whether they are charged, polar molecules or uncharged, no-polar compounds (Ahmedna *et al.*, 2004). However, at elevated activation temperature, the activated carbon yield is reduced due to the increased devolatilization rate of the sample. Ahmad and Alrozi (2010) found that the KOH further facilitates the decomposition of char during pyrolysis as the C-O-C and C-C bonds breaking thus lower the activated carbon yield. Tan *et al.* (2008b) also observed the similar trend where less coconut husk activated carbon yield obtained at higher activation temperature.

Activation time is able to influence the activated carbon prepared as prolong activation time would entail in opening an enlargement of the pores, therefore, enhanced the adsorption of dyes (Lua and Yang, 2004). Nonetheless, it does depend on requirement of specific activated carbon application, because prolong the activation time might cause continuous pore enlargement. Zhang *et al.*, (2004) found that the longer activation time resulted in greater adsorption capacity of oak activated carbon (OAC). The surface area and pore volume for 1 hour activation time were much less than those upon 2 hour activation time. Valix *et al.* (2008) also found the activation reaction began to dominate the structural development above 3 to 5 hours. At longer activation time, the apparent pore structure collapse and contribute to increase in ash content. However, as activation time longer, activated carbon yield were expected to be low due to devolatilization process.

IR plays an important role in creating and widening the pores in the activated carbon, thus contributes to the increase in surface area and adsorption capacity (Adinata *et al.*, 2007). Intercalation of chemical used onto carbon surface appeared to be responsible for the drastic expansion of the carbon material and hence the creation of a large surface area and high pore volume. Tan *et al.* (2008a) observed that the development of coconut husk into mesoporous activated carbon with relatively larger surface area ($1940 \text{ m}^2 \text{ g}^{-1}$) and total pore volume which comparable to commercial activated carbon.

2.5 Optimization of preparation conditions of activated carbon

The optimization of activated carbon preparation conditions is important in order to produce activated carbon with high adsorption capacity. Response surface methodology (RSM) is a collection statistical technique that is useful for modeling

and analysis purpose in which response of interest is influenced by several variables and the objective is to optimize this response. RSM contains three stages; (i) design and experiments, (ii) response modeling through regression, and (iii) optimization (Myers and Montgomery, 1995). A standard RSM design called central composite design (CCD) is commonly used to optimize the effective parameters with a minimum number of experiments, as well as to analyze the interactions between the parameters.

RSM been widely used for the optimization of activated carbon production from various precursors such as jatropha hull (Xin-Hui *et al.*, 2011), mangosteen peel (Ahmad and Alrozi, 2010), coconut husk (Tan *et al.*, 2008b), coconut shell (Gratiso *et al.*, 2008), and fly ash (Ravikumar *et al.*, 2007). By using RSM, Tan *et al.* (2008b) found that the optimized conditions for preparation of coconut husk based activated carbon for MB removal were at activation temperature, activation time and IR of 816°C, 1 h and 3.9, respectively. While Ravikumar *et al.* (2007) observed the optimum hybrid adsorbent (carbon and fly ash) preparation conditions for reactive red dye removal were at pH, temperature, particle size and time of 10.8, 59.52°C, 0.052 mm and 395 minutes, respectively. Xin-Hui *et al.* (2011) verified that the optimum conditions for preparation of jathropa hull based activated carbon at activation temperature, activation time and steam flow rate of 900°C, 18.82 min and 5 g/min, respectively, which lead in iodine adsorption of 979 mg/g and carbon yield of 16%.

2.6 Characterization of activated carbon

The pore characteristics of activated carbons are important in determining the adsorption performance of the activated carbon. Characterizations of activated

carbon comprise of activated carbon yield, surface area characteristics, surface morphology, proximate analysis and surface chemistry.

2.6.1 Activated carbon yield

The activated carbon yield is calculated based on the following equation:

$$\text{yield(\%)} = \frac{w_c}{w_0} \times 100 \quad (2.2)$$

where w_c and w_0 are the dry weight of final activated carbon (g) and the dry weight of precursor (g), respectively. Generally, carbon yield is found to decrease with increase in activation temperature because of carbon burn-off by elimination reaction at high temperature.

2.6.2 Surface area and pore characteristics

The surface area and the porosity are important characteristics in determining the adsorption capacity of the activated carbon. Surface area and pore characteristic of activated carbons normally determined by nitrogen (N_2) adsorption-desorption isotherms. This can be done with the method of Brunauer, Emmett and Teller (BET) which determine the surface area of any material. The method operates by measuring the quantity of nitrogen adsorbed onto or desorbed from a solid sample at different equilibrium vapor pressures at 77 K. The total pore volume is determined from the quantity of gas adsorbed at a relative pressure of 0.98. Generally, higher surface area is an indication of the existence of significant amount of porosity (Guo *et al.*, 2009). Bello *et al.* (2011) found that the activation process promotes the formation of mesopore and enhance surface area of the activated carbon. Table 2.3 summarizes surface area, total pore volumes and adsorbate for activated carbons produced from various precursors.

Table 2.3 Physical characteristics of activated carbon produced from various precursors

Precursors	S_{BET} (m^2/g)	V_T (cm^3/g)	Adsorbate	Reference
Cocoa pod husk	502.7	0.504	Remazol brilliant violet 5R	(Bello <i>et al.</i> , 2011)
Globe artichoke leaves	1745.0	0.450	Methylene blue	(Benadjemia <i>et al.</i> , 2011)
Rice straw	1154	0.670	Methylene blue	(Gao <i>et al.</i> , 2011)
Olive stones	1218	0.600	-	(Yakout and El-Deen, 2011)
Bamboo	1335	0.625	Methylene blue	(Liu <i>et al.</i> , 2010)
Coconut shell	1026.0	0.576	Phenol	(Mohd Din <i>et al.</i> , 2009)
Vetiver roots	1272	1.91	Methylene blue	(Altenor <i>et al.</i> , 2009)
Peach stone	1298.0	0.828	Methylene blue	(Attia <i>et al.</i> , 2008)

V_T : Total pore volume

The classification of pore size in activated carbons are divided into three; micropores ($d < 2$ nm), mesopores ($2 < d < 50$ nm) and macropores ($d > 50$ nm). The pore size of activated carbon defines its adsorptive properties. Small pore size will not trap large adsorbate molecules and vice versa, whether they are charged, polar molecules or uncharged, non-polar compounds (Ioannidou and Zabanitou, 2007).

2.6.3 Surface morphology

Scanning Electron Microscopy (SEM) is used to study the surface morphology of the activated carbon. SEM analysis identifies the pore structure, surface structure and pore arrangement of samples. Numerous studies have been carried out for determining the surface attributes for activated carbon by researchers. Vijayaraghavan *et al.* (2009) found that the examined activated carbon derived from saw dust was relatively porous, with wide ranging cracks. While Xin Hui *et al.* (2011) observed presence of macro and mesoporous jathropa hull activated carbon indicated by small pores which having well developed pore network using SEM images. Plate 2.1 displays the SEM images of the mangosteen peel (MP), char and

MP activated carbon (Ahmad and Alrozi, 2010). The precursor's surface textures (Plate 2.1(a)) were rough, uneven, undulating and very little pores were presence. After carbonization process, some irregular holes and pores were developed and detected on the surfaces of char (Plate 2.1(b)) due to the sudden burst of the thermal expansion from pyrolysis. From plate 2.1 (c), it was observed that homogeneous type pores structure were well distributed on the surface of the MP activated carbon. The SEM images succeed in revealing well-developed pores and mesoporous structure of MP activated carbon.

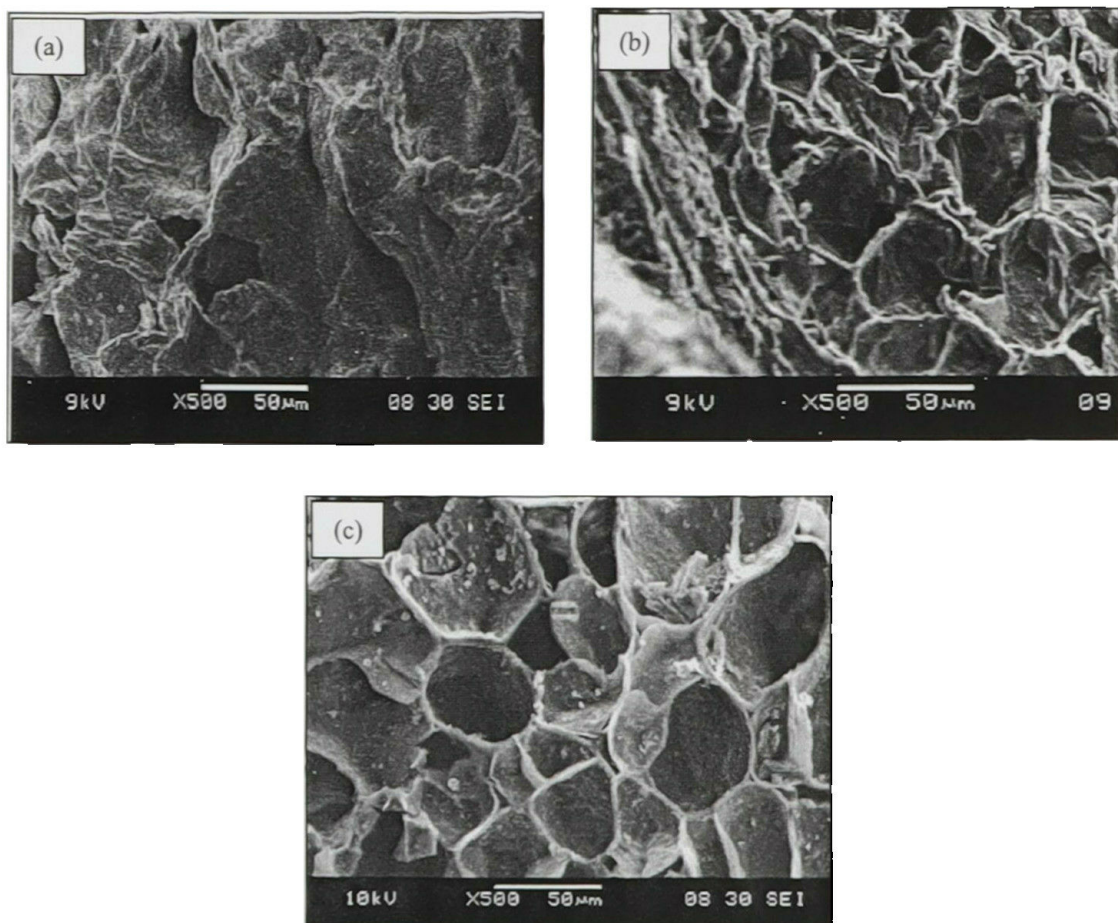


Plate 2.2 Scanning electron micrographs; (a) MP; (b) MP char; and (c) MP activated carbon (magnifications: 500x) (Ahmad and Alrozi, 2010).

2.6.4 Proximate analysis

Proximate analysis reveals the fixed carbon, ash, moisture and volatiles content of the samples. Proximate analysis is generally carried out by using simultaneous thermogravimetric analyzer (STA). Many literatures reported the moisture and volatiles content of the samples decreased significantly due to thermal effect. Bello *et al.* (2011) found that fixed carbon content of activated carbon derived from cocoa pod husk before and after treatment were increased (19.3-75.4%). This is due to pyrolytic effect at high temperature where most of the organic substances have been degraded into gaseous. During carbonization process, the excess volatile removed, thus explaining the decline in volatile content. Further removal occurred during activation which applied high temperature, thus removed much more volatile. Valix *et al.* (2008) observed chemically carbonized bagasse lost 63.5% of volatile materials in comparison to 5% lost by thermal carbonization. Nahil and Williams (2010) also observed shows the proximate analysis of the acrylic textile waste material and the chars produced at different final pyrolysis temperatures. The results indicate that there is a slight reduction in moisture content of the char samples as the pyrolysis temperature was increased. The volatile matter decreased and fixed carbon contents and ash increased with increasing pyrolysis temperature.

2.6.5 Surface chemistry

Fourier transform infrared (FTIR) spectroscopy is conducted to study the surface chemistry by identifying the presence of functional groups on the samples surface. The FTIR analysis confirms the regular formation of functional groups with gasification process. Valix *et al.* (2008) reported that the heteroatom can reside within the carbon layers forming heterocyclic rings, or bonded to edges and corners

of the aromatic rings or carbon defect positions. The carbon atoms retaining these groups have unsaturated valences that modify the surface characteristics and surface behavior of these carbon. Table 2.4 summarizes FTIR spectrum band assignments of pistachio-nut shell activated carbon (PNAC). FTIR analysis reveals functional groups presence on the PNAC surface and contributes to adsorption process.

Table 2.4 FTIR spectrum band assignments for pistachio-nut shell activated carbon (Lua and Yang, 2004)

Band number (cm ⁻¹)	Assignment
3366, 3435, 3362, 3397	$\nu(\text{O-H})$ vibration in hydroxyl group
2924	$\nu(\text{C-H})$ vibration in alkanes, alkyl groups
2918	$\nu(\text{C-H})$ vibration in aromatics group
2553	$\nu(\text{O-H})$ vibration in carboxylic acid group
2132, 2332	$\nu(\text{C}\equiv\text{C})$ vibration in alkyne group
1736, 1654	$\nu(\text{C=O})$ vibration in carbonyl group
1696	$\nu(\text{C=O})$ vibration in carboxylate group
1643	$\nu(\text{C=C})$ vibration in alkenes group
1586, 1505, 1428, 1566	$\nu(\text{C=C})$ vibration in aromatics group
1380, 1465	$\delta(\text{C-H})$ vibration in alkanes, alkyl groups
1332, 1374, 1396	$\nu(\text{C-O})$ vibration in carboxylate group
1300–900	$\nu(\text{C-O})$ vibration in esters, ether or phenol groups
897, 883, 875, 833, 829	$\gamma(\text{C-H})$ vibration in benzene derivatives
817, 750, 660, 669, 650	$\gamma(\text{O-H})$ vibration

2.7 Adsorption isotherm

Adsorption is usually described by the amount of adsorbate on the adsorbent as a function of its pressure (if gas) or concentration (if liquid) at constant temperature. The isotherm indicates how the adsorption molecules distribute between the liquid phase and the solid phase as the adsorption process reaches an equilibrium state. It is important to establish the most appropriate adsorption isotherm for different adsorbent system for purpose of designing the adsorption system (Gimbert *et al.*, 2008).

Generally, isotherm models such as Langmuir, Freundlich, Temkins, Koble-Corrigan, Toth, Sips, Vieth-Sladek, Radke-Prausnitz, and Bruoers-Sotolongo are used to describe the adsorption system. The isotherm models are utilized to fit the experimental equilibrium data. Non-linear regression method had been chosen to estimate the isotherm parameters. Microsoft spreadsheet with Solver add-in is able to determine the isotherm parameters by minimizing the respective coefficient of determination between experimental data and isotherm (Kumar, 2007). Microsoft Excel contains the SOLVER function, ideally suited to fitting data with non-linear function via iterative algorithm. SOLVER minimized the sum of the squared between data points and the function describing the data. The analysis of fitting degree of isotherm with the experimental data was represents by coefficient of determination, R^2 (Karadag *et al.*, 2007). The values vary from 0 to 1, whereas the closest R^2 to unity and the lowest % error values represents suitable parameter to correlate the adsorption behavior (Kumar and Sinavesan, 2006).

2.7.1 Langmuir isotherm

Langmuir model assumes that the adsorption process does not proceed beyond monolayer coverage. All the sites available on the adsorbent surface are equivalent and the surface is uniform. Basically, once the adsorbate is attached on the site, no further adsorption can take place at that site, Langmuir isotherm equation is given as (Langmuir, 1918):

$$q_e = \frac{Q_o K_L C_e}{1 + K_L C_e} \quad (2.3)$$

where C_e is the equilibrium concentration of the adsorbate (mg/L), q_e is the amount of adsorbate adsorbed per unit mass of adsorbent (mg/g), Q_o is the maximum monolayer adsorption capacity of the adsorbent (mg/g) and K_L is the Langmuir